DOI: 10.1093/brain/awg277 Advanced Access publication August 22, 2003 *Brain* (2003), **126,** 2667–2681

Gene expression profile of neurodegeneration induced by α_{1B}-adrenergic receptor overactivity: NMDA/$GABA_A$ dysregulation and apoptosis

June Yun,[1] Robert J. Gaivin,[1] D. F. McCune,[1] Attaporn Boongird,[2] Robert S. Papay,[1] Zhong Ying,[2] Pedro J. Gonzalez-Cabrera,[1] Imad Najm[2] and Dianne M. Perez[1]

[1]*Department of Molecular Cardiology, Lerner Research Institute and* [2]*Department of Neurology, The Cleveland Clinic Foundation, Cleveland, OH, USA*

Correspondence to: Dianne M. Perez, Department of Molecular Cardiology, Lerner Research Institute, Cleveland Clinic Foundation, 9500 Euclid Avenue, Cleveland, OH 44195, USA
E-mail: perezd@ccf.org

Summary

The α_1-adrenergic receptors (α_1ARs) play an important role in mediating sympathetic neurotransmission in peripheral organ systems; however, central α_1ARs are not well characterized. Additionally, due to the lack of sufficiently subtype-selective drugs or high avidity antibodies, the contribution of each α_1AR subtype to various central functions is currently unclear. Transcription regulation through α_1AR subtypes in the CNS is also unknown. Of interest, transgenic mice that systemically overexpress the α_{1B}AR show central symptoms that include age-progressive impaired mobility, neurodegeneration and susceptibility to epileptic seizure. To investigate the molecular basis of this phenotype, oligonucleotide microarray studies of whole brains of various ages were carried out to compare gene expression profiles between transgenic and normal brains. The results indicated changes in expression of apoptotic, calcium regulatory, neurodegenerative and genes involved in neurotransmission. Defects in regulation of intracellular calcium are known to play a role in cell death; thus, these genes may provide clues as to the molecular basis of α_{1B}AR-induced neurodegeneration. Epilepsy is a disorder that can be caused by an imbalance between excitatory (e.g. glutamate) and inhibitory (e.g. GABA) signals. Microarray analysis of transgenic brains showed increased *N*-methyl-D-aspartate (NMDA) receptors and decreased $GABA_A$, which were confirmed with immunohistochemistry, western blot and radioligand binding studies. The α_{1B}AR also co-localized with the glutamatergic distribution, suggesting a glutamate imbalance as a molecular rationale for the epileptic seizures.

Keywords: adrenergic; microarray; NMDA; GABA; transgenic

Abbreviations: α_1AR = α_1-adrenergic receptor; EGFP = enhanced green fluorescent protein; EST = expressed sequence tag; Ig = immunoglobulin; IHC = immunohistochemistry; MM = mismatched; NMDA = *N*-methyl-D-aspartate; NT = non-transgenic; PBS = phosphate-buffered saline; PM = perfectly matched; T = transgenic; TBS = Tris-buffered saline; TGF-β = transforming growth factor-β; WT = wild-type

Introduction

The α_1-adrenergic receptors (α_1ARs) are members of the superfamily of G protein-coupled receptors that mediate the effects of the endogenous catecholamines adrenaline and noradrenaline. The α_1ARs are classified into three subtypes (α_{1A}, α_{1B} and α_{1D}) based on molecular cloning and differing affinities for agonists and antagonists (Cotecchia *et al*., 1988; Lomasney *et al*., 1991; Perez *et al*., 1991, 1994; Graham *et al*., 1996). All three α_1AR subtypes transduce their signals intracellularly primarily via coupling of the receptor to the G_q pathway (Guarino *et al*., 1996), leading to the activation of downstream signalling molecules such as protein kinase C and the mobilization of calcium. α_1ARs participate in a number of physiological processes that are essential in the maintenance of homeostasis, including the regulation of blood pressure and cardiac contractility in the cardiovascular system, as well as sodium reabsorption and glucose metabolism in the kidney and liver, respectively (García-Sáinz *et al*., 1999).

In the CNS, although α_1AR density in the brain is equal to or exceeds that of other adrenergic receptors, the central

functions of these receptors remain unclear. Previous studies, however, indicate that α_1ARs are postsynaptic and are involved in the regulation of several central functions including synaptic transmission, plasticity, motor activity, as well as attention and memory. For example, α_1AR activation is thought to attenuate the excitability of pyramidal neurons in the hippocampus (Mynlieff and Dunwiddie, 1988), whereas in areas of the cerebral cortex, α_1AR activation potentiates excitation in response to glutamate or acetylcholine (Mouradian *et al*., 1991). α_1AR activation is primarily excitatory in regions such as the reticular thalamic nuclei, dorsal raphe and spiny motor neurons, largely due to decreased potassium conductance (McCormick *et al*., 1991). Open field activity assessments also showed that activation of central α_1ARs enhances locomotor activity, whereas α_1AR-selective blockers depressed motor activity (Stone *et al*., 1999). α_1ARs may also regulate brain functions via glial cells since activation of these receptors has been shown to induce calcium transients in astrocytes (Lerea and McCarthy, 1989). Recent studies from the α_{1B}AR knockout mouse suggest that this subtype may modulate dopamine release that affects the locomotor response to amphetamines (Drouin *et al*., 2002). While these limited functional responses to α_1 AR stimulation have begun to make inroads into α_1AR regulation of CNS function, there are no reports of any transcriptional regulation by α_1ARs in brain tissue whereby we can begin to analyse the mechanistic reasons for their activity.

Discerning the specific functional contribution of each α_1AR subtype in physiological systems, however, has been more challenging. Studies have been hindered primarily by the lack of sufficiently subtype-selective ligands, especially for the α_{1B}AR. To alleviate this constraint, we have examined the function of the α_{1B}AR in transgenic (T) mouse models that overexpress either wild-type (WT) or constitutively active forms of the α_{1B}AR in those tissues that endogenously express the receptor (Zuscik *et al*., 2000). These T mice exhibit a neurodegenerative phenotype accompanied by motor abnormalities that resemble the Parkinsonian disorder, multiple system atrophy. Additionally, the T brain also possesses increased levels of abnormally nitrated α-synuclein inclusion bodies that co-localize with oligodendrocytes and neurons, which is consistent with multiple system atrophy and other synucleinopathies (Papay *et al*., 2002). T mice also have epileptic seizures that can be induced starting at ~7 months of age and increasing in frequency and occurring spontaneously as the mice grow older (Zuscik *et al*., 2000). Furthermore, EEG studies indicate that these mice show abnormal ictal and interictal activity similar to human forms of epilepsy, indicating a potential role for α_{1B}ARs in the development of epileptogenicity (Kunieda *et al*., 2002). To identify the molecular mechanisms underlying these central effects of α_{1B}AR activation, we have carried out oligonucleotide microarray analyses on whole brains from T and age-matched normal non-transgenic (NT) control mice. Gene expression profiles were compared at three different ages to correlate gene expression changes with the onset or progression of symptoms. We have identified a number of disease-associated genes, including those involved in apoptosis and calcium/glutamate regulation, providing clues to the molecular bases underlying the central phenotypes observed in the T mice. In particular, we confirm a dysregulation in *N*-methyl-D-aspartate (NMDA) and GABA signals and apoptosis at the protein level, which may be responsible for the epileptic seizures and/or the neurodegeneration in the brains of the T mice.

Material and methods

Mice

The T mice (B6CBA) systemically overexpressing the α_{1B}AR have been described previously (Zuscik *et al*., 2000). Mice used in this study carried a transgene containing a cDNA coding for a constitutively active α_{1B}AR that carries three different mutations: C128F, A204V and A293E (Hwa *et al*., 1997). Systemic expression was achieved by using the murine α_{1B}AR gene promoter (Zuscik *et al*., 1999). Founder mice were identified and subsequent generations were genotyped by Southern analysis of genomic DNA isolated from tail biopsies. To show localization of the α_{1B}AR protein, we also constructed an enhanced green fluorescent protein (EGFP)-tagged WT α_{1B}AR in the same manner as above. The EGFP was added to the C-terminal tail of the WT α_{1B}AR. This investigation conforms to the *Guide for the Care and Use of Laboratory Animals* published by the US National Institutes of Health (NIH publication No. 85-23, revised 1996) and was approved by the Animal Research Committee of The Cleveland Clinic Foundation.

Preparation of cRNA and hybridization to oligonucleotide arrays

Poly(A)$^+$ RNA was isolated from whole brains of five or more T or NT mice each at three different ages, 2–4 months, 8–10 months and 12–18 months, generating six experimental groups: NT(2–4), T(2–4), NT(8–10), T(8–10), NT(12–18) and T(12–18). No difference in phenotype has been observed between male and female T mice, thus each T and NT group at each age contained the same number of male and female mice. RNA was isolated using the FastTrack 2.0 kit (Invitrogen, Carlsbad, CA). The RNAs isolated from individual mice were pooled within each group and double-stranded cDNA was synthesized from 1 μg of poly(A)$^+$ RNA using the Superscript Choice double-stranded cDNA synthesis kit (Gibco-BRL, Rockville, MD). Biotin-labelled cRNA was synthesized from the cDNA in an *in vitro* transcription reaction using the BioArray high yield RNA transcript labelling kit (Enzo Diagnostics, Farmingdale, NY). cRNAs were purified using the RNeasy Mini kit (Qiagen, Valencia, CA). Fragmentation of biotin-labelled cRNAs and subsequent hybridization to the oligonucleotide arrays were carried out by the Gene Expression Core Service at the Cleveland Clinic

Foundation. A 50 μg aliquot of biotin-labelled cRNA was then hybridized to the MGU74Av2 oligonucleotide array (Affymetrix, Santa Clara, CA), which represents 12 656 known murine genes and expressed sequence tags (ESTs) from Build 74 of the UniGene database. Each cRNA sample was hybridized to two microarrays and two analyses were carried out for each experimental group. Detection of gene expression changes was determined using Affymetrix software. Briefly, each gene or EST was represented on the chip by ~16 pairs of perfectly matched (PM) and mismatched (MM) oligonucleotides. PM–MM pairs differed by only a single base pair change in the MM oligo, and spanned distinct regions of the specified gene/EST represented by the probe set. The MM probes served as specificity controls to allow the direct subtraction of both background and cross-hybridization signals. The number of instances where the PM signal was greater than the MM signal was determined and the average of the logarithm of PM : MM was calculated. A matrix-based algorithm was then used to determine the presence or absence of each cRNA molecule. The abundance of each RNA transcript was then calculated by averaging the differences of PM–MM signals for each probe set after discarding the maximum, minimum and any outliers >3 SDs. Comparisons were then carried out between age-matched NT and T groups resulting in four possible combinations [i.e. NT(chip1) versus T(chip 1), NT(chip 1) versus T(chip2), NT(chip2) versus T(chip1) and NT(chip2) versus T(chip2)] at each age studied. Those transcripts that were found to be significantly increased or decreased in three of the four comparisons and exhibited an average fold change of 1.6 or greater were then included in data tables. This fold cut-off was determined by previous reports that revealed correlations between microarrays and Taqman PCR data at the 1.6- to1.8-fold threshold (Tan *et al*., 2002).

Northern analysis

Several of the genes that were identified as having increased or decreased transcript levels via microarray studies were examined by northern blot analyses. cDNA probes were isolated from IMAGE Consortium (Lawrence Livermore National Laboratory LLNL) ESTs obtained from the American Type Culture Collection: interferon-γ receptor 2 (cloneID: 4164791), insulin receptor subsrate 2 (cloneID: 3164252) and P-type ATPase (cloneID: 3385756). Probes were radiolabelled with [^{32}P]dCTP (6000 Ci/mmol; NEN, Boston, MA) using the random primed DNA labelling kit (Roche, Indianapolis, IN). Equal amounts of poly(A)$^+$ RNA (5 μg) used in the microarray experiments were loaded onto 0.8 % agarose–formaldehyde gels, transferred to nitrocellulose and hybridized to the appropriate probes. Band density was determined by scanning densitometry using NIH image software.

Western blot analyses

Individual whole brains were homogenized in 4 ml of M-Per™ mammalian protein extraction reagent (Pierce, Rockford, IL), supplemented with 0.2 TIU/ml aprotinin, 1 mM EDTA, 2 μM leupeptin, 1 mM phenylmethylsulfonyl fluoride (PMSF) and 60 μM benzamidine. Homogenates were incubated on ice for 20 min then centrifuged for 10 min at maximum speed at 4°C. The supernatant was collected as total cell lysate and used for subsequent western blots. Protein concentrations were measured with the Bio-Rad (Hercules, CA) protein assay kit, using bovine serum albumin (BSA) as a standard. Equal amounts of protein were solubilized in sample buffer [65.5 mM Tris–HCl pH 6.8, 2% sodium dodecyl sulfate (SDS), 10% glycerol, 0.001% bromophenol blue, 5% β-mercaptoethanol], electrophoresed on a 4–15% gradient Tris–HCl SDS–polyacrylamide gel (Bio-Rad) and transferred to nitrocellulose membranes. Membranes were blocked for 1 h at room temperature with 5% non-fat dry milk in Tris-buffered saline (TBS) with 0.05% Tween-20 (TBS-T), and incubated with a rabbit polyclonal antibody directed against NR1 (0.2 μg/ml; Chemicon, Temecula, CA) or NR2A/B (0.2 μg/ml; Chemicon) for 1 h at room temperature. Blots were washed and subsequently incubated with secondary goat anti-rabbit immunoglobulin (Ig)G conjugated to horseradish peroxidase (1 : 5000; Jackson Immunologicals, West Chester, PA). Proteins were visualized using enhanced chemiluminescence (Pierce).

Immunohistochemistry

For NR1 and activated caspase 3 immunohistochemistry (IHC) experiments, mice were deeply anaesthetized with pentobarbital (100 mg/kg, intraperitonaeally), then transcardially perfused with 20 ml of ice-cold heparin in phosphate-buffered saline (PBS; 10 U/ml), followed by 100 ml of 4% paraformaldehyde in 0.1 M Na_2HPO_4 buffer pH 7.0. Brains were removed and post-fixed in the same fixative for 3 h. After fixation, brains were cryoprotected in 20% sucrose overnight and sectioned on a cryostat (16 μm in thickness) the following day. Sections were transferred onto electrostatic slides, dried at room temperature then stored at –20°C until use. For experiments, sections were thawed, re-hydrated with PBS, then antigen retrieval was carried out in 10 mM citric acid pH 6.0 for 10 min in a microwave oven. Sections were then incubated successively with 10% normal goat serum for 1 h at room temperature, anti-NR1 (0.7 μg/ml; Chemicon) or anti-activated caspase 3 (1 : 100; Cell Signaling) in PBS containing 1% normal goat serum and 0.03% Triton X-100 overnight at 4°C, biotinylated goat anti-rabbit for 1 h at room temperature, 3% H_2O_2 in PBS for 20 min at room temperature, and avidin-biotinylated horseradish peroxidase complex (Vectastain Elite ABC kit, Vector Laboratories, Burlingame, CA) for 30 min at room temperature. Immunoreactions were visualized with 3,3′-diaminobenzidine (DAB; Vector Laboratories).

For NR2A/B IHC experiments, serial 30 μm thick coronal sections were collected and processed for immunostaining with antibody for NR2A/B (rabbit IgG, 0.5 μg/ml; Chemicon AB 1548, Temecula, CA). The sections were placed in

individual 3 ml tissue culture wells containing 0.05 M TBS pH 7.6. TBS was used as the rinsing buffer between each step throughout the IHC staining procedure: (i) 5 min in 3% H_2O_2/10% methanol in TBS; (ii) 60 min in a blocking solution of 1.5% normal goat serum in TBS; (iii) overnight at room temperature in primary antibody diluted in TBS; (iv) 35 min in diluted biotinylated goat anti-rabbit IgG; and (v) 60 min in a solution of excess avidin and biotinylated horseradish peroxidase (ABC kit, Vector Laboratories). In order to visualize the immunoreactive complex, the sections were reacted for 8 min in 0.05% DAB and 0.01% H_2O_2 in TBS. Control experiments for IHC were performed by omission of primary antibody using the same staining protocol as mentioned above; no specific IHC staining was seen in the absence of specific primary antibody.

For localization of the α_{1B}AR protein, sections were washed in PBS and blocked by incubation in PBS containing 0.3% Triton X-100 and 2% BSA. The α_{1B}AR tagged receptor was identified with a rabbit anti-GFP (Chemicon) at 1 : 2500. Bound primary antibodies were detected by incubation with fluorescein isothiocyanate (FITC)-coupled anti-rabbit IgG at 1 : 2500. Slides were then treated for 1 h in 10 mM $CuSO_4$ in 50 mM ammonium acetate pH 5.0 to reduce autofluorescence due to lipofuscin. Slides were mounted in Vectashield mounting medium (Vector Laboratories). Sections were analysed on a confocal laser-scanning microscope (Model Aristoplan; Leica, Inc., Deerfield, IL). Confocal images represent optical sections of ~1 μm axial resolution. Single images represented an average of 16 line scans of the chosen field.

Radioligand binding studies

GABA$_A$

Membranes were prepared as described (Enna and McCarson, 1998). Briefly, brains were homogenized with a polytron in ice-cold 50 mM Tris-citrate buffer pH 7.1 then centrifuged for 10 min at 50 000 *g*. The pellet was resuspended in Tris-citrate buffer, and re-centrifuged as described. This wash was repeated five more times to remove endogenous GABA, and the final pellet was resuspended in 10–15 ml of Tris-citrate buffer. For saturation binding studies, membranes (400 μg) were incubated with increasing concentrations of [^{3}H]muscimol (20–300 nM; NEN Life Sciences, Boston, MA), and non-specific binding was measured in the presence of 0.1 mM bicuculline (Sigma, St Louis, MO). Reactions were carried out for 30 min at 4°C, then terminated by addition of 3 ml of Tris-citrate buffer.

GABA$_B$

Membranes were prepared essentially as described (Enna and McCarson, 1998). Briefly, whole brains were homogenized in ice-cold buffer (50 mM Tris–HCl, 2.5 mM $CaCl_2$ pH 7.4). The homogenate was then centrifuged at 20 000 *g* for 20 min. The pellet was resuspended in homogenization buffer and centrifuged as above; this process was repeated three more times. The final membrane pellet was resuspended in 10–15 ml of the same buffer. For saturation binding studies, membranes (400 μg) were incubated with increasing concentrations of [^{3}H]baclofen (10–100 nM, NEN Life Sciences), and non-specific binding was measured in the presence of 1 mM saclofen (Tocris, Ellisville, MO). Reactions were incubated for 10 min at 25°C, then terminated by addition of ice-cold Tris-$CaCl_2$ buffer.

NMDA

Brain membranes were prepared as described (Ferkany, 1999). Briefly, brains were homogenized in ice-cold 0.32 M sucrose and the sample centrifuged for 10 min at 2000 *g*. The supernatant was collected, fresh sucrose was added to the sample, and the sample was centrifuged for 20 min at 12 500 *g*. The pellet was resuspended in deionized water and homogenized. The resulting homogenate was then centrifuged for 20 min at 8000 *g*. The buffy coat and supernatant were resuspended by inversion, and the sample was centrifuged for 10 min at 40 000 *g*. The pellet was resuspended in 2% Tris–HCl pH 7.4, and centrifuged as in the previous step. The pellet was washed in the same manner four more times and stored at –70°C until the day of the assay. Membranes were resuspended in 50 mM Tris–HCl, 100 mM potassium thiocyanate buffer and homogenized. The homogenate was centrifuged for 10 min at 40 000 *g* and resuspended in Tris-potassium thiocyanate buffer. This step was repeated five more times and the final pellet was resuspended in 10–15 ml of the Tris-potassium thiocyanate buffer. The binding experiments were carried out with increasing concentrations of [^{3}H]CGP39653 (5–40 nM; Perkin Elmer Life Sciences) and 400 μg of membrane protein. Non-specific binding was measured in the presence of 0.01 mM (±)CPP (Sigma). The assay was terminated with Tris-potassium thiocyanate buffer.

For competition experiments, membranes were labelled with 70 pM [^{125}I]MK801 (Perkin Elmer Life Sciences) and incubated with increasing concentrations of the NR2B-selective antagonist, ifenprodil (0.01 nM–1 mM; Sigma). Binding was carried out for 60 min at 4°C. The final volume for all binding reactions was 500 μl, and all binding reactions were terminated by addition of 3 ml of the appropriate buffer. Reactions were filtered through GF/B filters with a Brandel cell harvester. Filters were washed three times with the appropriate buffer, placed in 20 ml of scintillation cocktail, and counted on a scintillation counter. B_{max} and K_d values were obtained with non-linear regression analyses using GraphPad Prism (San Diego, CA). For competition studies, curves were fitted to a two-site model and the percentage of high and low affinity sites was calculated using GraphPad Prism.

Table 1 *Expression of genes involved in pathways of neurodegeneration in T brains*

Encoded protein (accession no.)	Age (months)		
	2–4	8–10	12–18
Glutamate/calcium regulation			
Calcium-sensing receptor (AF022252)	+2.8 ± 0.5	NC	NC
Calmodulin (M27844)	+1.7 ± 0.08	NC	NC
Ryanodine receptor3 (X83934)	–2.0 ± 0.5	NC	NC
Store-operated calcium channel (U73625)	–5.7 ± 2.6	NC	–2.5 ± 0.2
CaM kinase II (plasticity; X14836)	–11.0 ± 0.5	+4.5 ± 0.4	+3.9 ± 0.5
Plasma membrane Ca^{2+}-ATPase (AF053471)	NC	+5.2 ± 1	+6.1 ± 0.9
L-type Ca(2+) channel (U73487)	NC	+2.7 ± 0.06	+2.6 ± 0.1
NMDA receptor R1 (D10028)	NC	+2.3 ± 0.1	+2.8 ± 0.1
AMPA receptor α3 (AB022342)	NC	+2.0 ± 0.1	NC
Glutamate decarboxylase (D42051)	NC	NC	+2.7 ± 0.1
Guanylate kinase (U53514)	NC	NC	+2.2 ± 0.05
$GABA_A$ receptor α1 (X61430)	NC	NC	–1.9 ± 0.03
$GABA_A$ receptor γ1 (X55272)	NC	NC	–3.0 ± 0.1
Apoptotic			
Bik-like killer (AF048838)	+6.1 ± 2	NC	NC
Met proto-oncogene (Y00671)	+5.6 ± 2.3	NC	NC
TGF-β (AJ009862)	+5.0 ± 1.0	NC	NC
CD40 ligand (X65453)	+4.2 ± 0.6	NC	NC
Superoxide dismutase 1 (M35725)	+3.2 ± 0.03	NC	NC
JunB (U20735)	NC	+7.0 ± 0.4	NC
Insulin-like growth factor receptor 1 (AF056187)	NC	+1.7 ± 0.03	NC
TIA (U00689)	NC	–1.7 ± 0.06	–2.2 ± 0.03
Activin receptor, type I (L15436)	NC	NC	–2.6 ± 0.3
PITSLRE kinase (L37092)	NC	NC	–2.8 ± 0.5
Neurodegenerative			
α-Tubulin, inclusion bodies (M13441)	+1.7 ± 0.06	NC	NC
Tau, inclusion bodies (M18776)	+1.6 ± 0.05	NC	NC
Apoliprotein E, plaque development (D00466)	+1.6 ± 0.03	NC	NC
Ubiquitin conjugating enzyme (X92664)	–1.8 ± 0.2	NC	NC
LR11, apoE receptor (AB015790)	NC	NC	+5.8 ± 0.3
Niemann–Pick type C1 (AF003348)	NC	NC	+1.8 ± 0.03
Apbb2, plaque formation (U70210)	NC	NC	–3.3 ± 0.2

Data are expressed as gene expression fold changes ± SEM of a four-way comparison as described in Material and methods. NC = no change; Accession numbers are from GenBank.

Results

Gene expression profile

To identify genes that may contribute to the neurological phenotype observed in T mice, gene expression profiles of whole brains from T mice were compared with expression profiles of NT control brains at three different ages: 2–4 months (before disease manifestation), 8–10 months (symptoms begin and worsen) and 12–18 months (diseased state). Age-matched controls negated gene expression changes due to ageing of the mice. Based on our criteria and after ESTs that did not encode a protein were removed, overexpression of α_{1B}ARs resulted in the expression changes of 88 genes in 2- to 4-month-old mice (0.6%), 62 genes in 8- to 10-month-old mice (0.5%), and 122 genes in 12- to 18-month-old mice (1.0%). The remaining genes were grouped into functional classifications: glutamate/calcium regulation, apoptotic and neurodegenerative proteins (Table 1); synaptic and structural proteins (Table 2); proliferative/growth and immune proteins (Table 3); and proteins involved in signalling and modifying or transcription and translation (Table 4). Gene expression changes in each table are ranked from highest expression levels to lowest, starting with 2- to 4-month-old mice, then 8- to 10-month-old and, finally, 12- to 18-month-old mice. Of particular interest, expression of genes coding for protein products that are involved in regulation of excitatory or inhibitory signals, e.g. glutamate, GABA or calcium regulation, were found to be primarily changed in 8 month or older T brains as compared with younger T brains (Table 1). In general, genes associated with apoptosis or neurodegeneration (Table 1) were differentially expressed in younger T, whereas genes involved in growth or gene regulation were found to be changing in 8 month or older T brains (Tables 3 and 4).

Confirmation of microarray data

To confirm the gene expression changes observed in the microarray experiments, northern blotting analysis was

Table 2 *Expression of genes involved in structural aspects of cellular function in T brains*

Encoded protein (accession no.)	Age (months)		
	2–4	8–10	12–18
Synaptic/vesicular transport			
Interleukin 7 receptor (M29697)	+4.3 ± 0.6	NC	NC
Neurotensin receptor (U51908)	+2.1 ± 0.06	NC	NC
Complexin 2 (D38613)	+2.1 ± 0.06	+1.8 ± 0.04	NC
Synaptophysin (X95818)	–1.8 ± 0.06	NC	NC
Kinesin heavy chain 1a (D29951)	–2.1 ± 0.1	NC	+2.5 ± 0
Kv4.2 (AF107780)	–3.3 ± 0.8	NC	NC
Syntaxin 1B (D29743)	–3.5 ± 1.0	NC	NC
Girk1 (D45022)	–5.1 ± 1.4	NC	NC
Kv1.6 (M96688)	–6.7 ± 0.7	NC	NC
Secretory protein 23 (D12713)	–7.0 ± 1.1	–4.2 ± 0.03	–4.4 ± 0.2
Insulin-like growth factor receptor 2 (U04710)	–9.3 ± 1.7	NC	NC
Kinesin heavy chain 5c (AF067180)	NC	+3.4 ± 0.2	NC
SNARE (X61455)	NC	+3.0 ± 0.04	+3.6 ± 0.09
Kv1.1 (Y00305)	NC	+2.3 ± 0.06	+2.8 ± 0.1
ER81 (L10426)	NC	+1.7 ± 0.04	+2.8 ± 0.05
Kinesin heavy chain 5b (U86090)	NC	–1.9 ± 0.1	–2.0 ± 0.1
Synapsin IIb (AF096867)	NC	NC	+2.9 ± 0.1
MB-IRK2 (X80417)	NC	NC	+2.8 ± 0.03
Trans-Golgi network protein 2 (D50032)	NC	NC	–5.4 ± 0.3
Kinesin member c2 (U92949)	NC	NC	–2.6 ± 0.1
RAB7 (X89650)	NC	NC	–1.7 ± 0.03
Golga 5 (AB016784)	NC	NC	–1.8 ± 0.1
Synaptotagmin XI (AB026808)	NC	NC	–1.9 ± 0.04
Adhesion/structural			
Involucrin (L28819)	+4.7 ± 0.06	NC	NC
Cofilin (L29468)	–1.8 ± 0.3	NC	NC
Matrin3 (AB009275)	–2.4 ± 0.2	NC	–2.4 ± 0.1
Prefoldin (Y17393)	–2.8 ± 0.7	NC	NC
Eph receptor (X79082)	–3.1 ± 0.5	NC	NC
Myelin-associated oligodendrocytic (U81317)	–3.4 ± 0.5	NC	NC
Tissue factor pathway inhibitor (AF004833)	–4.0 ± 0.4	NC	NC
Robo1 (Y17793)	–4.8 ± 0.8	NC	NC
Wasp (U42471)	–5.0 ± 0.4	NC	NC
P-type ATPase I (U75321)	NC	+8.2 ± 1.1	+7.7 ± 0.3
Pten (U92437)	NC	+2.5 ± 0.1	+4.3 ± 0.09
Prosaposin (AF037437)	NC	NC	+4.5 ± 0.3
Microtubule-associated protein 2 (M21041)	NC	NC	+3.6 ± 0.2
Glial cell adhesion molecule (X16646)	NC	NC	+2.2 ± 0.2
Ankyrin 3	NC	NC	+2.1 ± 0.01
Cadherin 10 (U69137)	NC	NC	–1.7 ± 0.1
Marcks (M60474)	NC	NC	–1.7 ± 0.05
Fibronectin receptor β (integrin, X15202)	NC	NC	–2.2 ± 0.07

Data are expressed as gene expression fold changes ± SEM of a four-way comparison as described in Material and methods. NC = no change; Accession numbers are from GenBank.

carried out with several genes whose expression was found to be increased (P-type ATPase and insulin receptor substrate 2) or decreased (interferon-γ receptor 2) at the indicated ages (Fig. 1). Generally, qualitative changes (positive or negative expression) were conserved between the microarray and northern experiments; however, quantitative fold changes were greater in the microarray data compared with the northern blots. This is consistent with previous reports (Yun *et al*., 2003) in which microarray analysis may be more sensitive than northern analysis.

Protein levels of NR1 and NR2A/B

One of the more interesting subsets of gene expression changes in T brains, especially in the 8 month or older mice, were those involved in regulating intracellular calcium or glutamate levels. Expression of several glutamate receptor genes such as the major NMDA receptor subunit NR1 were increased in T brains compared with NT brains (see Table 1). To determine whether the gene expression changes were apparent at the protein level, we compared the protein levels of the NMDA receptor subunits, NR1 and NR2A/B, in whole

Table 3 *Expression of genes involved in growth and immune response in T brains*

Encoded protein (accession no.)	Age (months)		
	2–4	8–10	12–18
Growth			
Gsg2 (D87326)	+5.3 ± 1.1	NC	NC
Inhibin B (U89840)	+5.2 ± 0.9	NC	NC
Pro-opiomelanocortin α (J00612)	+3.8 ± 0.2	NC	+5.4 ± 0.5
Brain neurotensin receptor 2 (U51908)	+2.1 ± 0.06	NC	NC
Calmodulin (M27844)	+1.7 ± 0.09	NC	NC
Jun kinase (AB005664)	–2.0 ± 0.4	NC	NC
Carboxypeptidase D (D85391)	NC	+5.0 ± 0.5	+3.6 ± 0.4
Casein kinase II (U51866)	NC	+2.8 ± 0.7	+4.9 ± 0.2
Pcm1 (AF039021)	NC	+2.4 ± 0.04	+2.3 ± 0.03
Prolactin (X04418)	NC	NC	+53.7 ± 10
Growth hormone (X02891)	NC	NC	+16.6 ± 0.2
Insulin receptor substrate 2 (AF090738)	NC	NC	+7.7 ± 0.2
Bone morphogenetic protein receptor II (AF003942)	NC	NC	+4.1 ± 0.2
Glycoprotein hormone (J00643)	NC	NC	+3.8 ± 0.08
Fibroblast growth factor, inducible (U42384)	NC	NC	+3.7 ± 0.4
Endothelin receptor, B (U32329)	NC	NC	+3.5 ± 0.4
Ten m4 (AB025413)	NC	NC	+1.9 ± 0.03
Brain-derived neurotrophic factor (X55573)	NC	NC	+1.8 ± 0.03
Thyroid hormone receptor (U09504)	NC	NC	–1.8 ± 0.04
CTP synthase (U49350)	NC	NC	–2.2 ± 0.2
Activin receptor, type I (L15436)	NC	NC	–2.6 ± 0.3
Immune/defence			
Igκ variable (AB007986)	+5.0 ± 0.8	NC	NC
Interleukin 4 (X035320	+4.6 ± 0.7	NC	NC
Stress-induced phosphoprotein (U27830)	–1.9 ± 0.09	NC	NC
Ly49E, natural killer cell receptor (U10091)	–3.6 ± 0.7	NC	NC
Tec tyrosine kinase (X55663)	–5.6 ± 0.2	NC	NC
Immune suppressor factor TJ6 (M31226)	NC	+1.8 ± 0.03	NC
Heat shock protein70 (M20567)	NC	–1.7 ± 0.2	–1.9 ± 0.2
Igκ chain, C region (M80423)	NC	–3.2 ± 0.3	NC
Interferon γ receptor (U69599)	NC	–3.3 ± 0.2	NC
C1q-related factor (AF095155)	NC	NC	+2.6 ± 0.08
Natural killer-enhancing factor B (U20611)	NC	NC	+2.3 ± 0.04
Complement C1q (X58861)	NC	NC	+2.2 ± 0.05
Heat shock protein 40 (AB028272)	NC	NC	+1.8 ± 0.08
Interferon β (V00756)	NC	NC	–1.8 ± 0.2
Paraoxonase 2 (L48514)	NC	NC	–2.2 ± 0.07
Orosomucoid 2 (M12566)	NC	NC	–2.3 ± 0.3

Data are expressed as gene expression fold changes ± SEM of a four-way comparison as described in Material and methods. NC = no change; Accession numbers are from GenBank.

brain cell lysates of 2- to 4-month-old and 8- to 10-month-old mice via western blotting (Fig. 2). The 8- to 10 month-old T brains showed ~2-fold higher levels of NR1 subunit, which was consistent with the ~2-fold increased levels observed in the microarray studies (Fig. 2B). Levels of NR2A and NR2B subunits were detected using an antibody that does not distinguish between these two subunits. Western blotting experiments indicated that T brains also showed ~1.5-fold higher levels of the NR2A/B subunits than age-matched NT brains (Fig. 2). Increased protein levels of NMDA receptor subunits were also detected in 2- to 4-month-old T brains (Fig. 2A).

Immunolocalization of NR1 and NR2A/B

To identify specific brain regions expressing increased levels of NR1 and NR2A/B, IHC experiments were performed. T brains at both young and old age points showed increased levels of the NR1 protein in the cerebral cortex (Fig. 3A and B) and hippocampus (not shown) as well as in other brain regions including the cerebellum and thalamus (not shown). Increased staining was observed in neuronal cell bodies as well as in the dendritic processes of the cortex in T brains. Increased NR2A/B staining was also dramatically increased in the cortex and hippocampus regions of the T brains (Fig. 3C–F).

Table 4 *Expression of genes involved in signalling and regulation of transcription and translation in T brains*

Encoded protein (accession no.)	Age (months)		
	2–4	8–10	12–18
Signalling/modifying enzymes			
Spink3 protease inhibitor (X06342)	+5.2 ± 0.8	NC	NC
Mast cell protease (M57401)	+3.8 ± 2.3	NC	NC
Phosphatidylinositol glycan, class F (D50264)	+2.6 ± 0.5	NC	NC
SPAK, Ste 20 kinase (AF099988)	–1.7 ± 0.08	NC	NC
Protein phosphatase 1B (D45859)	–1.9 ± 0.1	NC	NC
Rgs4 (AB004315)	–2.1 ± 0.3	NC	NC
Diacylglycerol kinase α (AF085219)	–4.4 ± 0.4	NC	NC
Srpk2 (AB006036)	–7.4 ± 0.4	NC	NC
Dystrobrevin (Z79787)	NC	+2.3 ± 0.2	NC
RANGAP1 (U08110)	NC	+2.0 ± 0.03	NC
cAMP-dependent kinase inhibitor (M63554)	NC	–1.9 ± 0.06	–2.0 ± 0.06
14-3-3 γ (AF058799)	NC	NC	+4.5 ± 0.06
Rgs5 (U67188)	NC	NC	+2.5 ± 0.1
EF hands protein phosphatase (AF023458)	NC	NC	+1.7 ± 0.1
Tiam1 (U05245)	NC	NC	–2.0 ± 0.1
Prp4 kinase (AF033663)	NC	NC	–2.3 ± 0.3
Transcription/translation regulatory			
TEA (U51743)	+7.3 ± 1.3	NC	NC
Nuclear respiratory factor 2 (M74515)	+6.0 ± 0.7	NC	NC
Mcm4 (D26089)	+5.2 ± 1.6	NC	NC
Pbx3b (AF020200)	+1.8 ± 0.06	NC	NC
Pr264 (X98511)	+1.8 ± 0.05	NC	NC
HMG-17 (X12944)	–2.3 ± 0.1	NC	NC
Smad3 (AB008192)	–4.1 ± 1.4	NC	NC
Acidic nuclear phosphoprotein 32 (U73478)	NC	+9.0 ± 0.2	NC
RCK RNA helicase (AF038995)	NC	+4.9 ± 0.2	+5.6 ± 0.1
NFAT4 (D85612)	NC	+2.5 ± 0.3	+2.4 ± 0.2
Protein kinase inhibitor p58 (U284230	NC	+2.3 ± 0.2	+3.5 ± 0.2
AP-2 (X78197)	NC	+1.9 ± 0.2	NC
STAT6 (L47650)	NC	–2.1 ± 0.06	NC
Pbx1b (L27453)	NC	NC	+3.0 ± 0.2
Ppar γ-binding protein (AF000294)	NC	NC	+2.9 ± 0.1
Fos (V00727)	NC	NC	+2.1 ± 0.06
NeuroD (U28068)	NC	NC	+2.1 ± 0.03
Nuclear factor I/B (Y07685)	NC	NC	–1.7 ± 0.03
NeuroD2 (D83507)	NC	NC	–3.0 ± 0.04
Protein L, hnrnp (AB009392)	NC	NC	–1.7 ± 0.2
Stat1 (U06924)	NC	NC	–1.8 ± 0.16
Nnx3 (AF091096)	NC	NC	–2.0 ± 0.09
Replication factor C (X72711)	NC	NC	–2.3 ± 0.2
HNF-3, brain factor 1 (U36760)	NC	NC	-2.4 ± 0.2

Data are expressed as gene expression fold changes ± SEM of a four-way comparison as described in Material and methods. NC = no change; Accession numbers are from GenBank.

Radioligand binding studies

Radioligand binding experiments were carried out to determine NMDA, $GABA_A$ and $GABA_B$ receptor densities (Table 5). $GABA_B$ receptor levels were not significantly different in both 2- to 4- and 10- to 24-month-old T brains when compared with their age-matched controls. $GABA_A$ receptor levels, however, were significantly decreased by ~50% in 10- to 24-month-old T brains (Table 5), which corresponded to the decrease in transcript levels as observed in the microarray studies (see Table 1). Increased NMDA receptor levels (3- to 7-fold) were also confirmed in both 2- to 4- and 10- to 24-month-old T brains compared with age-matched control brains. No significant differences in affinity (K_d) was detected in T brains for all ligands used in the saturation experiments. To determine whether the T mice increased the NR2A or NR2B subunits of the NMDA receptor, competition ligand binding studies were performed using [^{125}I]MK801 and the NR2B-selective antagonist, ifenprodil. T mice had an increase in the percentage of high affinity sites (Fig. 4, Table 5) compared with age-matched controls.

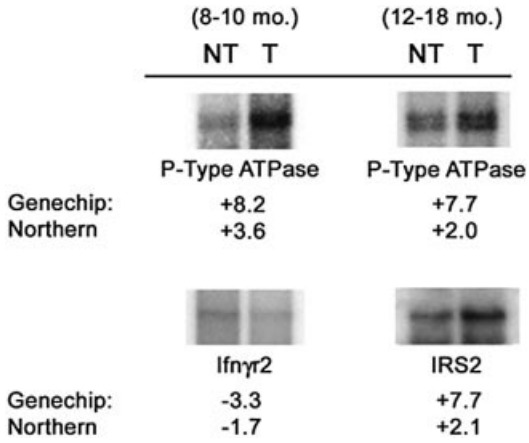

Fig. 1 Northern blot analysis. As confirmation of microarray results, northern blotting experiments were carried out with mRNA samples from NT and T brains using cDNA probes against the indicated genes that were differentially expressed at each age examined. Northern analyses were carried out using 5 μg of the poly(A)$^+$ RNA that was used in the microarray experiments for each age group. Fold changes in intensity of each gene in T brains are indicated, as are fold changes measured from northern experiments (using NIH image software).

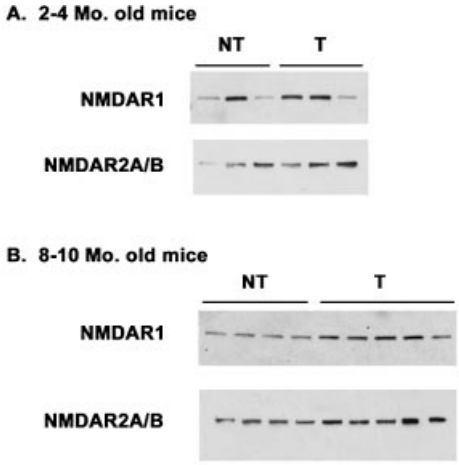

Fig. 2 Western blot analysis of NMDA receptor subunits in (**A**) 2- to 4-month-old and (**B**) 8- to 10-month-old brains. Individual NT and T brains were homogenized and total cell lysates were run on denaturing SDS–polyacrylamide gels. Both NR1 and NR2A/B levels were found to be increased in 2- to 4- and 8- to 10-month-old T mice by ~2-fold compared with age-matched NT control mice.

Confirmation of apoptosis

Since many different types of apoptotic genes were upregulating in the younger mice and some of these pathways appeared to be regulated through transforming growth factor-β (TGF-β), we chose to use antibodies against the activated form of caspase 3, a pathway converging effector of apoptosis for the TGF-β pathway. T brains from 2- to 3-month-old mice had high levels of activated caspase 3 in the white matter tracts of the cerebellum (Fig. 5B), the corpus callosum and the myelinated tracts of the caudate/putamen (Fig. 5D). Upon higher magnification of the medulla, activated caspase 3 was seen only in the nuclei (Fig. 5F).

Localization of the α_{1B}AR to hippocampal and cerebral cortex regions

To determine if the α_{1B}AR protein is located in the same regions of the hippocampus and cerebral cortex that are also upregulating NMDA receptor subunits, we performed immunofluorescence studies on T mice expressing a WT α_{1B}AR tagged at the C-terminal tail with EGFP (Fig. 6). Due to the low endogenous expression of the T mice with this housekeeping promoter, the green fluorescent images were present but are very low intensity. Therefore, we employed an antibody against EGFP to visualize the receptor. The WT α_{1B}AR does have neurodegeneration (Zuscik *et al*., 2000) but is only present later in life. For the localization studies, we employed animals that were 2–3 months old. We found that the α_{1B}AR does indeed localize to regions that control the molecular areas of the dentate gyrus and hippocampal associational fibres, and regions of the cerebral cortex which correlate to the distribution of glutamatergic systems (Fig. 6).

Discussion

The functional roles of distinct α_1AR subtypes have remained relatively elusive primarily due to the lack of sufficiently powerful tools with which to study their functional differences. Thus to attempt to gain greater insight into the physiological contribution of α_{1B}ARs, we previously generated a mouse model that systemically overexpresses the α_{1B}AR (Zuscik *et al*., 2000). Interestingly, overactivity of the α_{1B}AR led to impaired hindlimb mobility that became apparent starting at 3 months and progressively worsened with age. Additionally, neurodegeneration was observed predominantly in the cerebellum and medulla, but progressed to virtually all brain areas as the mice grew older. By 7 months of age, T mice had epileptic seizures that could be induced by stresses (e.g. handling) that became spontaneous and more frequent as the mice grew older. To gain insight into the potential pathways that may be involved in initiating or propagating these symptoms, we have carried out microarray analyses of NT and T brains at various ages.

One class of genes that were differentially expressed in T brains were those involved in glutamate/calcium regulation (Table 1). Changes in the expression of these genes primarily occurred in 8 month or older T mice. Of note, genes coding for three different ionotropic glutamate receptor subunits, NR1, α-amino-3-hydroxy-5-methyl-4-isoxazole proprionic acid 1 (AMPA1) and AMPA3, were upregulated in older T brains. Similarly, mRNA levels of $GABA_A$ receptor subunits were also decreased in older T brains (Table 1). These changes coincided with the manifestation and progression of

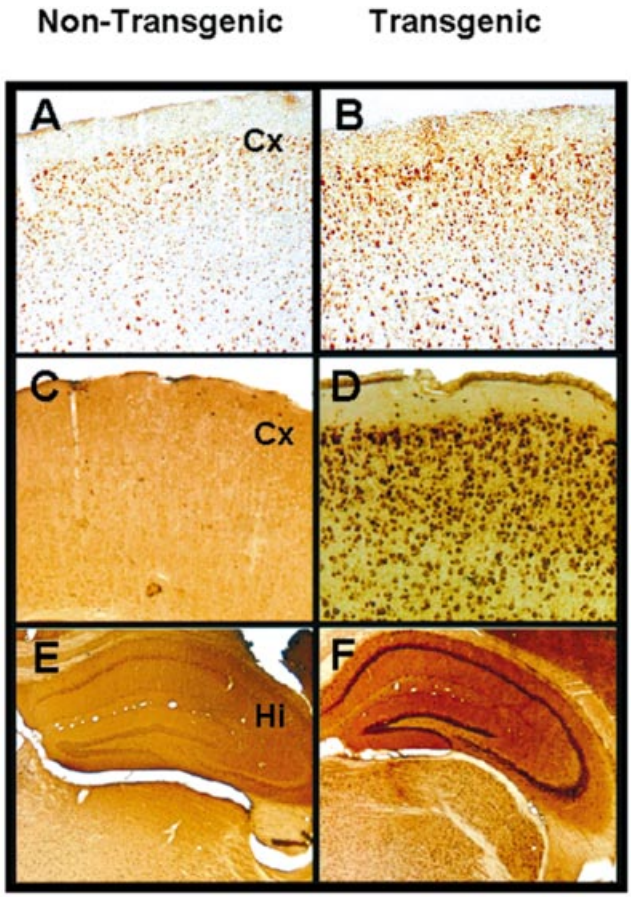

Fig. 3 NR1 and NR2A/B proteins were detected by immunohistochemistry in paraformaldehyde-fixed brain sections isolated from NT and T brains. Immunohistochemical localization of NMDA receptor subunit proteins is shown in 12- to 13-month-old brains. (**A**) NR1 staining in NT cortex; (**B**) NR1 staining in T cortex. Cortical staining of NR2A/B in (**C**) NT and (**D**) T brains; hippocampal staining of NR2A/B in (**E**) NT and (**F**) T brains. Cx = cortex; Hi = hippocampus.

epileptic seizures in the T mice and were confirmed by ligand binding (Table 5), western blotting (Fig. 2) and IHC (Fig. 3).

Glutamate is the major excitatory neurotransmitter of the CNS (Petralia *et al*., 1994). A key factor in the mechanism of epileptogenesis is the ratio of inhibitory versus excitatory synapses (Najm *et al*., 2001). Excessive excitation or inadequate inhibition results in seizures. Previous studies have indicated increased NMDA receptor binding in cortex of some human epilepsies (Geddes *et al*., 1990; McDonald *et al*., 1991) as well as increased mRNA levels of both NR1 and NR2 subunits in temporal lobe epilepsy patients in *in situ* hybridization experiments (Mathern *et al*., 1997). Additionally, previous studies also associated increased glutamatergic AMPA receptor density and mRNA expression with focal epileptic human cortex and epileptic hippocampus (McDonald *et al*., 1991; García-Ladona *et al*., 1994; Zilles *et al*., 1999).

For a functional NMDA receptor, the NR1 subunit must partner with one or more NR2 subunits. The various NR2

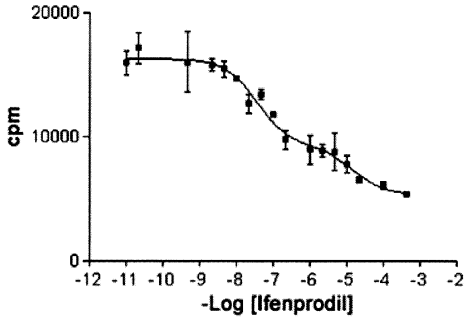

Fig. 4 Representative competition binding curve of ifenprodil at NMDA receptors in T brains. [^{125}I]MK801 is competed off with increasing concentrations of ifenprodil. The percentages of high and low affinity sites were determined by fitting the curve to a two-site model with Graphpad Prism. The percentage of high affinity sites which represent the NR2B subunit of the NMDA receptor was increased in T brains.

subunits, NR2A–D, are differentially expressed in a spatio-temporal manner. Embryonic and neonatal forebrains show relatively high levels of NR2B, with increasing NR2A levels from the time of birth through the second postnatal week. At this time, an adult expression pattern is reached (Takahashi *et al*., 1996). The NR2A/B subunit has previously been associated with epilepsy. Dysplastic cortical neurons express both NR1 and NR2A/B proteins; in contrast, non-dysplastic neurons express only NR1 proteins. The co-expression of NR1 and NR2A/B in dysplastic neurons suggests that heteromeric NR1–NR2A/B receptors in these neurons could contribute to focal seizure onset (Ying *et al*., 1999). IHC studies further indicate an increase in the densities of NR2A/B subunits in human epileptic cortex (Najm *et al*., 2000).

The NR2A/B subunit in our studies is likely to be the NR2B as determined by the competition ligand binding studies using the NR2B-selective ligand, ifenprodil (Fig. 4, Table 5). The identity of the NR2 subunit can be distinguished since recombinant NR1–NR2B receptors exhibit a 10- to 100-fold higher affinity for ifenprodil than NR1–NR2A receptors (Grimwood *et al*., 2000). T mice displayed an ~16% increase in the amount of high affinity sites for ifenprodil compared with age-matched normals. Since the increased NR2B may be highly localized to cortex and hippocampus (Fig. 3), ligand binding using whole brain membranes may not be as sensitive as using membranes from these distinct regions. Nonetheless, even under these conditions, the T brain displayed higher amounts of the NR2B subunits.

Our studies show an increase in NR1 and NR2A/B protein in whole brain lysates from T brains (Fig. 2). While there are differences in penetrance (two out of three samples are increasing), this result is consistent with previous data in which the seizure phenotype also has a 60% penetrance (Zuscik *et al*., 2000). Moreover, these increases in both NR1 and NR2A/B were detected in both the cortex and the hippocampus, two brain regions that are highly associated with epileptogenesis (Wahnschaffe *et al*., 1993). Radioligand binding studies further showed that T mice had increased

Table 5. *Radioligand binding analyis of $GABA_A$, $GABA_B$ and NMDA receptors in NT and T brains*

Age of mouse (months)	$GABA_A$		$GABA_B$		NMDA	
2–4	B_{max} (pmol/mg)	K_d (nM)	B_{max} (pmol/mg)	K_d (nM)	B_{max} (pmol/mg)	K_d (pM)
NT	0.336 ± 0.06	210 ± 128	0.07 ± 0.02	72 ± 24	0.07 ± 0.02	15 ± 6.4
T	0.304 ± 0.08	130 ± 25	0.03 ± 0.02	61 ± 27	0.483 ± 0.1*	24 ± 9.3
10–24						
NT	0.258 ± 0.06	138 ± 38	0.02 ± 0.002	42 ± 19.5	0.107 ± 0.01	11 ± 3
T	0.132 ± 0.02**	87 ± 14	0.02 ± 0.006	54 ± 15	0.300 ± 0.1**	74 ± 40
Ifenprodil competition						
10–24	–Log K_H	–Log K_L	% High affinity			
NT	7.9 ± 0.3	5.1 ± 0.5	45 ± 1			
T	7.6 ± 0.2	4.7 ± 0.3	61 ± 4*			

Membranes were isolated from NT and T brains and saturation binding studies were carried out as indicated in Material and methods. $GABA_A$ receptor density was measured using increasing concentrations of [^{3}H]muscimol and cold bicuculline. $GABA_B$ receptor density was measured using increasing concentrations of [^{3}H]baclofen in the presence of cold saclofen. Maximum NMDA receptor-binding sites (B_{max}) was measured with increasing concentrations of [^{3}H]CGP-39653 in the presence of cold (±)CPP; n = 4–6 independent curves. NMDA receptor-binding sites were significantly increased in both 2- to 4- and 10- to 24-month-old T brains. Additionally, $GABA_A$ receptor-binding sites were significantly decreased in 10- to 24-month-old T brains. Competition binding experiments were performed using 70 pM [^{125}I]MK801 in the presence of increasing concentrations of ifenprodil (0.01 nM to 1 mM); n = 2–3 independent curves (*P = 0.02: **P = 0.03, Student's t test).

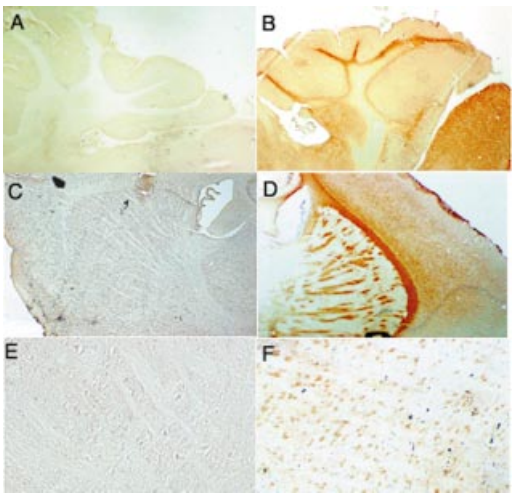

Fig. 5 Activated caspase 3 was detected in the white matter tracts of the cerebellum and corpus callosum and in the grey matter of the medulla in paraformaldehyde-fixed brain sections isolated from NT and T brains. IHC localization of activated caspase 3 protein is shown in 2- to 3-month-old brains. (**A**) NT cerebellum/medulla; (**B**) T cerebellum/medulla; (**C**) NT caudate putamen and corpus callosum; (**D**) T caudate putamen and corpus callosum; (**E**) NT medulla at higher magnification; (**F**) T medulla at higher magnification. T brains contained activated caspase 3 in the white matter tracts of the corpus callosum, the heavily myelinated tracts of the caudate/putamen and white matter of the cerebellum. T brains also contained activated caspase 3 in the grey matter of the medulla.

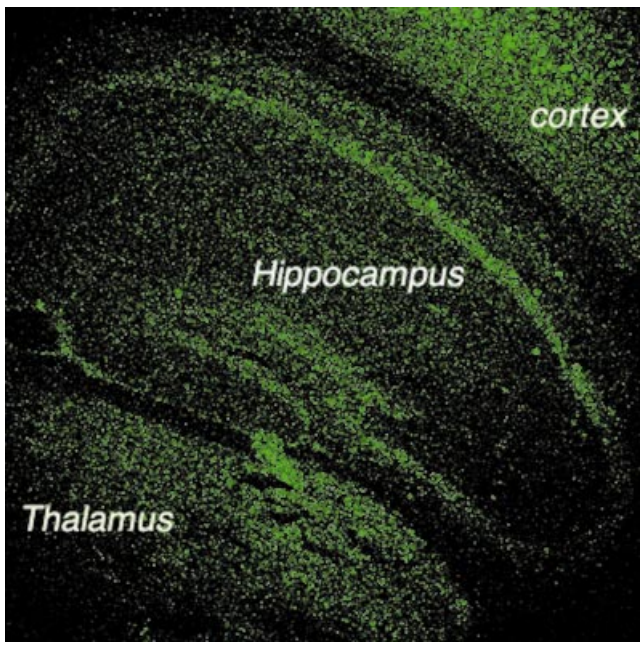

Fig. 6 Localization of the WT α_{1B}AR in the CA1–3 regions and dentate gyrus of the hippocampus and in the cerebral cortex in paraformaldehyde-fixed brain sections. T mice expressing an EGFP-tagged WT α_{1B}AR are used to show the localization of the receptor protein under the control of the same murine α_{1B}AR promoter as previously described (Zuscik *et al*., 2000). The receptor is visualized using an antibody against the EGFP protein and the sections are also washed in copper sulfate to reduce autofluorescence. The α_{1B}AR is localized to various domains of the hippocampus and cerebral cortex, consistent with the localization of the NMDA receptor.

membrane expression of NMDA receptors, confirming an increase in functional NMDA receptors in T brains, consistent with a state of excessive excitation. Overall, ~60% of the T mice tested showed increased NR2A/B levels via IHC and western studies, which is most probably due to the penetrance of the transgene.

Changes in gene expression that code for glutamate receptors responsible for excitatory signals were also accompanied by a decrease in mRNA of two $GABA_A$ receptor subunits which resulted in reduced $GABA_A$ receptor density as measured by receptor binding. The inter-regulation of the NMDA and GABA receptors is common since a homeostatic balance is needed to maintain proper neurotransmission. Fast synaptic inhibition is mediated primarily by the GABA neurotransmitter acting upon the $GABA_A$ receptors; therefore, decreased GABA transmission can also lead to a hyperexcitable state that results in epileptogenesis. While gene expression of glutamate decarboxylase does increase in the older T mice, this may be a compensatory mechanism to counteract the decreased $GABA_A$ signalling. Our results are consistent with previous findings, in which human epileptic patients and experimental epileptic models have also shown reduced or mutated $GABA_A$ receptors (Savic *et al*., 1988; McDonald *et al*., 1991; Kapur *et al*., 1994; DeLorey *et al*., 1998). α_1AR stimulation is known to excite the inhibitory GABAergic interneurons of the hippocampus (Bergles *et al*., 1996), but the α_1AR subtype remains unknown. While these results do not prove that the epilepsy in these T mice is mediated through the NMDA/GABA dysregulation, they are suggestive. T mice expressing an EGFP-tagged WT α_{1B}AR do indeed show that this receptor subtype is localized to areas co-existent with the glutamatergic and NMDA receptors, such as the CA1–3 regions and the dentate gyrus of the epileptic-prone hippocampus (Fig 6). Also consistent with epilepsy and distribution of the glutamatergic system is the localization of the α_{1B}AR to the neurons in the cerebral cortex. In fact, it seems that the areas that increased in NR1 and NR2B subunits (Fig 3) also co-express the α_{1B}AR (Fig 6). We are currently performing patch-clamp experiments in *in vitro* brain slices that include the hippocampal formation of the T mice.

Contrary to our findings, noradrenaline is known to be an anticonvulsant, and direct stimulation of α_1ARs shows anticonvulsant effects in many seizure models, including amygdala kindling (Löscher and Czuczwar, 1987), audiogenic (Yan *et al*., 1998) and spontaneous petit mal seizures (Micheletti *et al*., 1987). However, strychnine-induced convulsions in mice are potentiated by noradrenaline, possibly through α_1ARs (Amabeoku and Chandomba, 1994). Our findings indicate that chronic activation of the α_{1B}AR can lead to seizures through regulation of the NMDA and GABA receptors. Previous reports show that noradrenaline modulates NMDA (Kirkwood *et al*., 1999) and GABA signalling (Beani *et al*., 1986) in the cortex. However, our results are likely to be due to the secondary effects of neurodegeneration since glutamate dysregulation was a late-onset event.

Expression of genes with protein products involved in apoptosis and neurodegeneration was also found to be changed in T brains (Table 1). Pro-apoptotic proteins such as the Bik-like killer protein and TGF-β were upregulated in the 2- to 4-month-old T brains, indicating that apoptotic cell death begins early in life and may be mediated directly through α_{1B}AR stimulation. Previous TUNEL staining showed increased labelling of fragmented DNA in discrete T brain regions (Zuscik *et al*., 2000). A common effector of the TGF-β pathway is caspase 3. Using an antibody that recognizes only the activated form, immunostaining experiments in 2- to 3-month-old T brains show increased labelling of activated caspase 3 proteins (Fig 5), indicating caspase-mediated cell death in T brains. These findings are consistent with our previous microarray studies of T hearts (Yun *et al*., 2003), where TGF-β-mediated apoptotic genes were differentially expressed in 2-month-old T hearts rather than older hearts. The large amount of white matter apoptosis is consistent with our original assessment that the neurodegenerative phenotype in this T mouse resembles the white matter disease caused by multiple system atrophy (Zuscik *et al*., 2000). Additionally, G protein-coupled receptor-mediated apoptosis has been shown previously to occur in the parathyroid hormone/parathyroid hormone-related protein signalling pathway via G_q/phospholipase C (PLC) signalling (Turner *et al*., 2000), which is the same pathway that is activated by the α_{1B}AR. Heart-targeted G_q overexpression also induced apoptosis (Adams *et al*., 1998). Because of the excitatory effects of glutamate transmission and the widespread expression of glutamate receptors in the mammalian CNS, glutamate neurotransmission has been implicated in the pathogenesis of a number of central defects including ischaemia, and neurodegenerative diseases, as well as epilepsy (Choi *et al*., 1990; Reynolds *et al*., 1994; Ulas *et al*., 1994; Glass and Dragunow, 1995). Thus excessive glutamate signalling could also be excitotoxic, contributing to the widespread neurodegeneration apparent in older T brains. On the other hand, the excessive activation of the α_{1B}AR itself could directly mediate the apoptosis.

α_{1B}AR activation also seems to regulate the expression of genes involved in synaptic or vesicular transport (Table 2). Proteins that are associated with neurotransmitter release include the synaptotagmins, SNARE and complexin, which are all involved in Ca^{2+}-dependent exocytosis and vesicle docking. Other regulated proteins include the synaptophysins, which form fusion channels to allow neurotransmitter release and the synapsins, which are responsible for regulating the reserve pool of synaptic vesicles (reviewed in Hou and Dahlström, 2000). Kinesin proteins that are involved in axonal transport of synaptic vesicles were also differentially expressed in T brains, which may indicate a significant role for α_{1B}ARs in the regulation of neurotransmitter release. In fact, previous studies showed that α_1AR activation is involved in a presynaptic reduction in glutamate release in the dentate gyrus (Scanziani *et al*., 1993) and may be involved in the release of noradrenaline (Murphy and Majewski, 1989; Forray *et al*., 1999). However, because there is little evidence for presynaptic α_1ARs, more experiments should be carried out to examine these potential actions further.

Knowledge of the transcriptional regulation by the α_1ARs is limited. α_1AR stimulation is well known to activate the

fetal gene programme in cardiac myocytes, such as β-myosin heavy chain and skeletal α-actin (Stewart *et al*., 1998). Activation of the transcription of c-fos and c-jun is also regulated by the α_1AR (Garcia-Sainz *et al*., 1998). In the brain, nothing is known about α_1AR effects on transcription let alone the role of the individual subtypes. To understand α_1AR subtype-specific gene transcription on a wide scale, we performed an oligonucleotide microarray study in transfected rat-1 fibroblasts, stably expressing each of the three α_1AR subtypes (Gonzalez-Cabrera *et al*, 2003). Common to all three subtypes were genes involved in transcriptional regulation such as c-Fos and c-Jun, and cytokines and growth factors. Fos did increase in the T brain (Table 4) as well as jun kinase (Table 3). Two genes that were specific to the α_{1B}AR subtype in the rat-1 fibroblasts that also changed in the T brains were tau and TGF-β. While the expression of many other gene families was conserved in the microarray studies of fibroblasts versus brain, the exact genes were different, which is likely to be due to cell type differences. For instance, in fibroblasts, STAT 3 was actively transcribed while, in the brain, STAT 6 and STAT 1 were affected. From the same T mice used in this study, a microarray analysis from the heart was also performed (Yun *et al*, 2003) which also showed TGF-β pathways being activated, along with apoptosis.

In summary, we have carried out a microarray study to identify the functional and transcriptional consequences of α_{1B}AR overexpression in the mouse brain. Notably, T mice that systemically overexpress a constitutively activated α_{1B}AR showed changes in the expression of genes involved in glutamate and calcium regulation, apoptosis and neurodegeneration, growth and synaptic vesicle transport. Age-dependent changes in gene expression were correlated with distinct neurological phenotypes observed in T mice, thus, this study should serve to aid in the delineation of the specific functional roles of α_{1B}ARs in the CNS.

Acknowledgements

This work was funded by RO1HL61438 (D.M.P.), a T32 HL07914 training grant in Vascular Cell Biology (J.Y.) and a local American Heart Association fellowship (P.J.G.-C.).

References

Adams JW, Sakata Y, Davis MG, Sah VP, Wang Y, Liggett SB, et al. Enhanced Gαq signaling: a common pathway mediates cardiac hypertrophy and apoptotic heart failure. Proc Natl Acad Sci USA 1998; 95: 10140–5.

Amabeoku G, Chandomba R. Strychnine-induced seizures in mice: the role of noradrenaline. Prog Neuropsychopharmacol Biol Psychiatry 1994; 18: 753–63.

Beani L, Tanganelli S, Antonelli T, Bianchi C. Noradrenergic modulation of cortical acetylcholine release is both direct and gamma-aminobutyric acid-mediated. J Pharmacol Exp Ther 1986; 236: 230–6.

Bergles DE, Doze VA, Madison DV, Smith SJ. Excitatory actions of norepinephrine on multiple classes of hippocampal CA1 interneurons. J Neurosci 1996; 16: 572–85.

Choi DW, Rothman SM. The role of glutamate neurotoxicity in hypoxic–ischemic neuronal death. Annu Rev Neurosci 1990; 13: 171–82.

Cotecchia S, Schwinn DA, Randall RR, Lefkowitz RJ, Caron MG, Kobilka BK. Molecular cloning and expression of the cDNA for the hamster alpha 1-adrenergic receptor. Proc Natl Acad Sci USA 1988; 85: 7159–63.

DeLorey TM, Handforth A, Anagnostaras SG, Homanics GE, Minassian BA, Asatourian A, et al. Mice lacking the beta3 subunit of the GABAA receptor have the epilepsy phenotype and many of the behavioral characteristics of Angelman syndrome. J Neurosci 1998; 18: 8505–14.

Drouin C, Darracq L, Trovero F, Blanc G, Glowinski J, Cotecchia S, et al. Alpha1b-adrenergic receptors control locomotor and rewarding effects of psychostimulants and opiates. J Neurosci 2002; 22: 2873–84.

Enna SJ, McCarson KE. Characterization of GABA receptors. In: Taylor GP, editor. Current protocols in pharmacology. New York: John Wiley; 1998. p. 1.7.1–18.

Ferkany JW. Characterization of wild-type excitatory amino acid ion channel receptors. In: Taylor GP, editor. Current protocols in pharmacology. New York: John Wiley; 1999. p. 1.14.1–12.

Forray MI, Bustos G, Gysling K. Noradrenaline inhibits glutamate release in the rat bed nucleus of the stria terminalis: in vivo microdialysis studies. J Neurosci Res 1999; 55: 311–20.

García-Ladona FJ, Palacios JM, Probst A, Wieser HG, Mengod G. Excitatory amino acid AMPA receptor mRNA localization in several regions of normal and neurological disease affected human brain—an in situ hybridization histochemistry study. Brain Res Mol Brain Res 1994; 21: 75–84.

Garcia-Sainz JA, Alcantara-Hernandez R, Vazquez-Prado J. Alpha1-adrenoceptor subtype activation increases proto-oncogene mRNA levels. Role of protein kinase C. Eur J Pharmacol 1998; 342: 311–7.

García-Sáinz JA, Vázquez-Prado J, Villalobos-Molina R. α_1-Adrenoceptors: subtypes, signaling, and roles in health and disease. Arch Med Res 1999; 30: 449–58.

Geddes JW, Cahan LD, Cooper SM, Kim RC, Choi BH, Cotman CW. Altered distribution of excitatory amino acid receptors in temporal lobe epilepsy. Exp Neurol 1990; 108: 214–20.

Glass M, Dragunow M. Neurochemical and morphological changes associated with human epilepsy. Brain Res Rev 1995; 21: 29–41.

Gonzalez-Cabrera PJ, Gaivin R, Yun J, Ross SA, Papay RS, McCune DF, et al. Genetic profiling of α_1-adrenergic receptor subtypes by oligonucleotide microarrays: coupling to interleukin-6 secretion but differences in STAT 3 phosphorylation and gp-130. Mol Pharmacol 2003; 63: 1104–16.

Graham RM, Perez DM, Hwa J, Piascik MT. α_1-Adrenergic receptor subtypes. Molecular structure, function and signaling. Circ Res 1996; 78: 737–49.

Grimwood S, Richards P, Murray F, Harrison N, Wingrove PB, Hutson PH. Characterisation of N-methyl-D-aspartate receptor-specific [(3)H]ifenprodil binding to recombinant human NR1a/NR2B receptors compared with native receptors in rodent brain membranes. J Neurochem 2000; 75: 2455–63.

Guarino RD, Perez DM, Piascik MT. Recent advances in the molecular pharmacology of the α_1-adrenergic receptors. Cell Signal 1996; 8: 323–33.

Hou X-E, Dahlström A. Synaptic vesicle proteins and neuronal plasticity in adrenergic neurons. Neurochem Res 2000; 25: 1275–300.

Hwa J, Gaivin RJ, Porter JE, Perez DM. Synergism of constitutive activity in α_1-adrenergic receptor activation. Biochemistry 1997; 36: 633–9.

Kapur J, Lothman EW, DeLorenzo RJ. Loss of GABAA receptors during partial status epilepticus. Neurology 1994; 44: 2407–8.

Kirkwood A, Rozas C, Kirkwood J, Perez F, Bear MF. Modulation of long-term synaptic depression in visual cortex by acetylcholine and norepinephrine. J Neurosci 1999; 19: 1599–609.

Kunieda T, Zuscik MJ, Boongird A, Perez DM, Lüders HO, Najm. IM. Systemic overexpression of the α_{1B}-adrenergic receptor in mice: an animal model of epilepsy. Epilepsia 2002; 43: 1324–9.

Lerea LS, McCarthy KD. Astroglial cells in vitro are heterogeneous with respect to expression of the α-adrenergic receptor. Glia 1989; 2: 135–47.

Lomasney JW, Cotecchia S, Lorenz W, Leung WY, Schwinn DA, Yang-Feng TL, et al. Molecular cloning and expression of the cDNA for the alpha 1A-adrenergic receptor. The gene for which is located on human chromosome 5. J Biol Chem 1991; 266: 6365–9.

Löscher W, Czuczwar SJ. Comparison of drugs with different selectivity for central alpha 1-and alpha 2-adrenoceptors in animal models of epilepsy. Epilepsy Res 1987; 1: 165–72.

Mathern GW, Pretorius JK, Kornblum HI, Mendoza D, Lozada A, Leite JP, et al. Human hippocampal AMPA and NMDA mRNA levels in temporal lobe epilepsy patients. Brain 1997; 120: 1937–59.

McCormick DA, Pape H-C, Williamson A. Actions of norepinephrine in the cerebral cortex and thalamus: implications for function of the central noradrenergic system. Prog Brain Res 1991; 88: 293–305.

McDonald JW, Garofalo EA, Hood T, Sackellares JC, Gilman S, McKeever PE, et al. Altered excitatory and inhibitory amino acid receptor binding in hippocampus of patients with temporal lobe epilepsy. Ann Neurol 1991; 29: 529–41.

Micheletti G, Warter JM, Marescaux C, Depaulis A, Tranchant C, Rumbach L, et al. Effects of drugs affecting noradrenergic neurotransmission in rats with spontaneous petit mal-like seizures. Eur J Pharmacol 1987; 135: 397–402.

Mouradian RD, Sessler FM, Waterhouse BD. Noradrenergic potentiation of excitatory transmitter action in cerebrocortical slices: evidence for mediation by an α receptor-linked second messenger pathway. Brain Res 1991; 546: 83–95.

Murphy TV, Majeswski H. Modulaion of noradrenaline release in slices of rat kidney cortex through α_1- and α_2-adrenoceptors. Eur J Pharmacol 1989; 169: 285–95.

Mynlieff M, Dunwiddie TV. Noradrenergic depression of synaptic responses in hippocampus of rat: evidence for mediation by alpha1-receptors. Neuropharmacology 1988; 27: 391–8.

Najm IM, Ying Z, Babb T, Mohamed A, Hadam J, LaPresto E, et al. Epileptogenicity correlated with increased N-methyl-D-aspartate receptor subunit NR2A/B in human focal cortical dysplasia. Epilepsia 2000; 41: 971–6.

Najm I, Ying Z, Janigro D. Mechanisms of epileptogenesis. Neurol Clin 2001; 19: 237–50.

Papay R, Zuscik MJ, Ross SA, Yun J, McCune DF, Gonzalez-Cabrera PJ, et al. Mice expressing the α_{1B}-adrenergic receptor induces a synucleinopathy with excessive tyrosine nitration but decreased phosphorylation. J Neurochem 2002; 83: 623–34.

Perez DM, Piascik MT, Graham RM. Solution-phase library screening for the identification of rare clones: isolation of an α_{1d}-adrenergic receptor cDNA. Mol Pharmacol 1991; 40: 876–83.

Perez DM, Piascik MT, Malik N, Gaivin RJ, Graham RM. Cloning, expression, and tissue distribution of the rat homolog of the bovine α_{1c}-adrenergic receptor provide evidence for its classification as the α_{1a}-subtype. Mol Pharmacol 1994; 46: 823–31.

Petralia RS, Yokotani N, Wenthold RJ. Light and electron microscope distribution of the NMDA receptor subunit NMDAR1 in the rat nervous system using a selective anti-peptide antibody. J Neurosci 1994; 14: 667–96.

Reynolds GP, Pearson SJ, Hutson PH. Deficit of [^{3}H]L-689,560 binding to the glycine site of the glutamate/NMDA receptor in the brain in Huntington's disease. J Neurol Sci 1994; 125: 46–9.

Savic I, Persson A, Roland P, Pauli S, Sedvall G, Widen L. In-vivo demonstration of reduced benzodiazepine receptor binding in human epileptic foci. Lancet 1988; 2: 863–6.

Scanziani M, Gähwiler BH, Thompson SM. Presynaptic inhibition of excitatory synaptic transmission mediated by α adrenergic receptors in area CA3 of the rat hippocampus *in vitro*. J Neurosci 1993; 13: 5393–401.

Stewart AF, Suzow J, Kubota T, Ueyama T, Chen HH. Transcription factor RTEF-1 mediates alpha1-adrenergic reactivation of the fetal gene program in cardiac myocytes. Circ Res 1998; 83: 43–9.

Stone EA, Zhang Y, Rosengarten H, Yeretsian J, Quartermain D. Brain alpha 1-adrenergic neurotransmission is necessary for behavioral activation to environmental change in mice. Neuroscience 1999; 94: 1245–52.

Takahashi T, Feldmeyer D, Suzuki N, Onodera K, Cull-Candy SG, Sakimura K, et al. Functional correlation of NMDA receptor epsilon subunits expression with the properties of single-channel and synaptic currents in the developing cerebellum. J Neurosci 1996; 16: 4376–82.

Tan F-L, Moravec CS, Li J, Apperson-Hansen C, McCarthy PM, Young JB, et al. The gene expression fingerprint of human heart failure. Proc Natl Acad Sci USA 2002; 99: 11387–92.

Turner PR, Mefford S, Christakos S, Nissenson RA. Apoptosis mediated by activation of the G protein-coupled receptor for parathyroid hormone (PTH)/PTH-related protein (PTHrP). Mol Endocrinol 2000; 14: 241–54.

Ulas J, Weihmuller FB, Brunner LC, Joyce JN, Marshall JF, Cotman CW. Selective increase on NMDA-sensitive glutamate binding in the striatum of Parkinson's disease, Alzheimer's disease, and mixed Parkinson's disease/Alzheimer's disease patients: an autoradiographic study. J Neurosci 1994; 14: 6317–24.

Wahnschaffe U, Ebert U, Löscher W. The effects of lesions of the posterior piriform cortex on amygdala kindling in the rat. Brain Res 1993; 615: 295–303.

Yan QS, Dailey JW, Steenbergen JL, Jobe PC. Anticonvulsant effect of enhancement of noradrenergic transmission in the superior colliculus in genetically epilepsy-prone rats (GEPRs): a microinjection study. Brain Res 1998; 780: 199–209.

Ying Z, Babb TL, Mikuni N, Najm I, Drazba J, Bingaman W. Selective coexpression of NMDAR2A/B and NMDAR1 subunit proteins in dysplastic neurons of human epileptic cortex. Exp Neurol 1999; 159: 409–18.

Yun J, Zuscik MJ, Gonzalez-Cabrera P, McCune DF, Ross SA, Gaivin R, et al. Gene expression profiling of α_{1B}-adrenergic receptor-induced cardiac hypertrophy by oligonucleotide arrays. Cardiovasc Res 2003; 57: 443–55.

Zilles K, Qü MS, Köhling R, Speckmann E-J. Ionotropic glutamate and GABA receptors in human epileptic neocortical tissue: quantitative in vitro receptor autoradiography. Neuroscience 1999; 94: 1051–61.

Zuscik MJ, Piascik MT, Perez DM. Cloning, cell-type specificity, and regulatory function of the mouse alpha(1B)-adrenergic receptor promoter. Mol Pharmacol 1999; 56: 1288–97.

Zuscik MJ, Sands S, Ross SA, Waugh DJJ, Gaivin RJ, Morilak D, et al. Overexpression of the α_b-adrenergic receptor causes apoptotic neurodegeneration: multiple system atrophy. Nat Med 2000; 6: 1388–94.

Received April 21, 2003.
Revised May 30, 2003. Accepted June 24, 2003